

Search for New Physics in Lepton + Photon + X Events with 305 pb⁻¹ of p \bar{p}

Collisions at $\sqrt{s}= 1.96$ TeV

(Dated: May 10, 2006)

We present results of a search for anomalous production of events containing a charged lepton (ℓ , either e or μ) and a photon (γ), both with high transverse momentum, accompanied by additional signatures, X, including missing transverse energy (\cancel{E}_T) and additional leptons and photons. We use the same kinematic selection criteria as in a previous CDF search, but with a substantially larger data set, 305 pb⁻¹, a $p\bar{p}$ collision energy of 1.96 TeV, and the upgraded CDF II detector. We find 42 $\ell\gamma\cancel{E}_T$ events versus a standard model expectation of 37.3 ± 5.4 events. The level of excess observed in Run I, 16 events with an expectation of 7.6 ± 0.7 events (corresponding to a 2.7σ effect), is not supported by the new data. In the signature of $\ell\ell\gamma + X$ we observe 31 events versus an expectation of 23.0 ± 2.7 events. In this sample we find no events with an extra photon or \cancel{E}_T and so find no events like the one $ee\gamma\cancel{E}_T$ event observed in Run I.

PACS numbers: 13.85.Rm, 12.60.Jv, 13.85.Qk, 14.80.Ly

In 1995 the CDF experiment, studying $p\bar{p}$ collisions at a center-of-mass energy of 1.8 TeV at the Fermilab Tevatron, using 86 pb⁻¹ of data, observed [1–3] an event consistent with the production of two energetic photons, two energetic electrons, and large missing transverse energy \cancel{E}_T [4]. This signature is predicted to be very rare in the standard model (SM) of particle physics [5], with the dominant contribution being from the production of four gauge bosons: two W bosons and two photons. The event raised theoretical interest, however, as the $\ell\ell\gamma\gamma$ signature is expected in some models of physics “beyond the standard model” such as gauge-mediated models of supersymmetry [6] or the production of a pair of excited electrons [7]. The detection of this event led to the de-

velopment of “signature-based” inclusive searches to cast a wider net: in this case one search for two photons + X ($\gamma\gamma + X$) [1–3], and a second for one lepton + one photon + X ($\ell\gamma + X$) [8–10], where X can be another charged lepton (e or μ), another γ , or \cancel{E}_T , plus any number of jets. If pairs of new particles were being created, these inclusive signatures could be sensitive to possible other decay modes, or the creation and decay of related new particles.

Neither Run I search revealed convincing evidence for new physics. However, in the $\ell\gamma + X$ search, the results were consistent with SM expectations in a number of channels with “the possible exception of photon-lepton events with large \cancel{E}_T , for which the observed total was

16 events and the SM expectation was 7.6 ± 0.7 events, corresponding in likelihood to a 2.7 sigma effect.” [9]. The Run I paper concluded: “However, an excess of events with 0.7% likelihood (equivalent to 2.7 standard deviations for a Gaussian distribution) in one subsample among the five studied is an interesting result, but it is not a compelling observation of new physics. We look forward to more data in the upcoming run of the Fermilab Tevatron.” [9]. In this Letter we report the results of repeating the $\ell\gamma + X$ search with the same kinematic selection criteria in a substantially larger data set, 305 ± 18 pb⁻¹, a higher $p\bar{p}$ collision energy, 1.96 TeV, and the CDF II detector [11].

The CDF II detector is a cylindrically symmetric spectrometer designed to study $p\bar{p}$ collisions at the Fermilab Tevatron based on the same solenoidal magnet and central calorimeters as the CDF I detector [12] from which it was upgraded. Because the analysis described here is intended to repeat the Run I search as closely as possible, we note especially the differences from the CDF I detector relevant to the detection of leptons, photons, and \cancel{E}_T . The tracking systems used to measure the momenta of charged particles have been replaced with a central outer tracker (COT) with smaller drift cells [13], and an enhanced system of silicon strip detectors [14]. The calorimeters in the regions [15] with pseudorapidity $|\eta| > 1$ have been replaced with a more compact scintillator-based design, retaining the projective geome-

try [16]. The central CMU, CMP, and CMX [17] muon systems are unchanged in design, but the coverage of the CMP and CMX muon systems has been extended by filling in gaps in φ [11]. The data presented here were taken between March 2002 and August 2004.

Events with a high transverse momentum (p_T) [4] lepton or photon are selected by a three-level trigger [11] that requires an event to have either a lepton with $p_T > 18$ GeV or a photon with $E_T > 25$ GeV within the central region, $|\eta| \lesssim 1.0$. The trigger system selects photon and electron candidates from clusters of energy in the central electromagnetic calorimeter. Electrons are further distinguished from photons by requiring the presence of a COT track pointing at the cluster. The muon trigger requires a COT track that extrapolates to a reconstructed track segment (“stub”) in the muon drift chambers.

We use the same kinematic event selection as in the Run I analysis: inclusive $\ell\gamma$ events are selected by requiring a central photon candidate with $E_T^\gamma > 25$ GeV, a central lepton candidate (e or μ) with $E_T^\ell > 25$ GeV passing the “tight” criteria listed below, and a point of origin along the beam-line not more than 60 cm from the center of the detector.

The identification of leptons and photons is essentially the same as in the Run I search [8], with only minor technical differences, mostly due to changes in the construction of the tracking system and end-plug calorimeters.

A muon candidate passing the “tight” cuts has the following properties: a) a well-measured track in the COT; b) energies deposited in the electromagnetic and hadron compartments of the calorimeter consistent with expectations; c) a muon “stub” track in the CMX detector or in both the CMU and CMP detectors [11] consistent with the extrapolated position of the COT track; and d) COT timing measurements consistent with a track from a $p\bar{p}$ collision and not from a cosmic ray. An electron candidate passing the “tight” selection has the following properties: a) a high-quality track with p_T of at least half the shower energy, unless the $E_T > 100$ GeV, in which case the p_T threshold is set to 25 GeV; b) a transverse shower profile consistent with an electron shower shape and that matches the extrapolated track position; c) a lateral sharing of energy in the two calorimeter towers containing the electron shower consistent with that expected; and d) minimal leakage into the hadron calorimeter [18].

Photon candidates are required to have no track with $p_T > 1$ GeV, and at most one track with $p_T < 1$ GeV, pointing at the calorimeter cluster; good profiles in both transverse dimensions at shower maximum; and minimal leakage into the hadron calorimeter [18].

To reduce background from photons or leptons from the decays of hadrons produced in jets, both the photon and the lepton in each event are required to be “isolated”. The E_T deposited in the calorimeter towers in a cone in

$\eta - \varphi$ space [15] of radius $R = 0.4$ around the photon or lepton position is summed, and the E_T due to the photon or lepton is subtracted. The remaining E_T in the cone is required to be less than $2.0 \text{ GeV} + 0.02 \times (E_T - 20 \text{ GeV})$ for a photon, or less than 10% of the E_T for electrons or p_T for muons. In addition, for photons the sum of the p_T of all COT tracks in the cone must be less than $2.0 \text{ GeV} + 0.005 \times E_T$.

Missing transverse energy \cancel{E}_T is calculated from the calorimeter tower energies in the region $|\eta| < 3.6$. Corrections are then made to the \cancel{E}_T for non-uniform calorimeter response [19] for jets with uncorrected $E_T > 15$ GeV and $\eta < 2.0$, and for muons with $p_T > 20$ GeV.

A total of 574 events, 508 inclusive $e\gamma$ and 66 inclusive $\mu\gamma$ candidates, pass the $\ell\gamma$ selection criteria. Of the 508 inclusive $e\gamma$ events, 397 have the electron and photon within 30° of back-to-back in φ , $\cancel{E}_T < 25$ GeV, and no additional leptons or photons. These are dominated by $Z^0 \rightarrow e^+e^-$ decays in which one of the electrons radiates a high- E_T photon while traversing the material inside the COT active volume, leading to the observation of an electron and a photon approximately back-to-back in φ , with an $e\gamma$ invariant mass close to the Z^0 mass.

We use W^\pm and Z^0 production as control samples to ensure that the efficiencies for high- p_T electrons and muons, as well as for \cancel{E}_T , are well understood. The photon control sample is constructed from the events in which one of the electrons radiates a high- E_T pho-

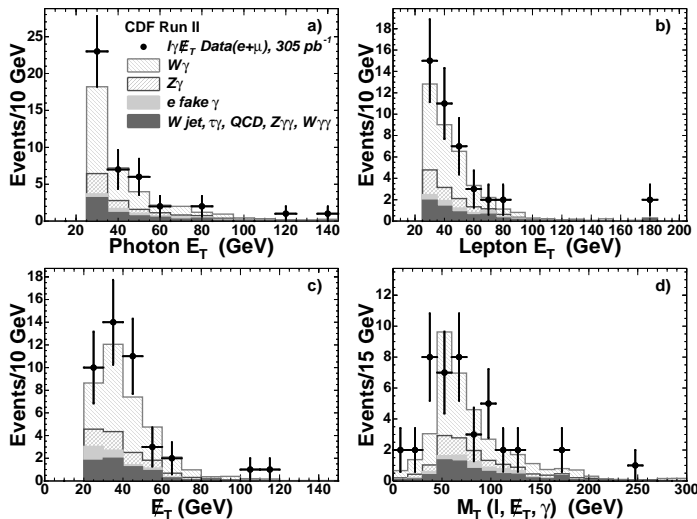


FIG. 1: The distributions for events in the $\ell\gamma\cancel{E}_T$ sample (points) in a) the E_T of the photon; b) the E_T of the lepton; c) the missing transverse energy, \cancel{E}_T ; and d) the transverse mass of the $\ell\gamma\cancel{E}_T$ system. The histograms show the expected SM contributions, including estimated backgrounds from misidentified photons and leptons.

ton, with an additional requirement that the $e\gamma$ invariant mass be within 10 GeV of the Z^0 mass.

The first search we perform is in the $\ell\gamma\cancel{E}_T + X$ subsample, defined by requiring that an event contain $\cancel{E}_T > 25$ GeV in addition to the photon and “tight” lepton. Of the 574 $\ell\gamma$ events, 25 $e\gamma\cancel{E}_T$ events and 17 $\mu\gamma\cancel{E}_T$ events pass the \cancel{E}_T requirement. Figure 1 shows the observed distributions summed over the $e\gamma\cancel{E}_T$ and $\mu\gamma\cancel{E}_T$ events in a) the E_T of the photon; b) the E_T of the lepton; c) the missing transverse energy, \cancel{E}_T ; and d) the transverse mass of the $\ell\gamma\cancel{E}_T$ system, where $M_T = [(\vec{E}_T^\ell + \vec{E}_T^\gamma + \vec{\cancel{E}}_T)^2 - (\vec{E}_T^\ell + \vec{E}_T^\gamma + \vec{\cancel{E}}_T)^2]^{1/2}$.

A second search, for the $\ell\ell\gamma + X$ signature, is constructed by requiring another electron or muon in addition to the “tight” lepton and the photon. The additional

muons are required to have $p_T > 20$ GeV and to satisfy at least one of two different sets of criteria: the same as those above for “tight” muons but with fewer hits required on the track, or a more stringent cut on track quality but no requirement that there be a matching “stub” in the muon systems. Additional central electrons are required to have $E_T > 20$ GeV and to satisfy the same criteria as tight central electrons but with a track requirement of only $p_T > 10$ GeV (rather than $0.5 \times E_T$), and no requirement on a shower maximum measurement or lateral energy sharing between calorimeter towers. Electrons in the end-plug calorimeters ($1.2 < |\eta| < 2.0$) are required to have $E_T > 15$ GeV, minimal leakage into the hadron calorimeter, a “track” containing at least 3 hits in the silicon tracking system, and a shower transverse shape consistent with that expected, with a centroid close to the extrapolated position of the track [20].

The $\ell\ell\gamma$ search criteria select 31 events (19 $ee\gamma$ and 12 $\mu\mu\gamma$) of the 574 $\ell\gamma$ events. No $e\mu\gamma$ events are observed. Figure 2 shows the observed distributions in a) the E_T of the photon; b) the E_T of the leptons; c) the 2-body mass of the dilepton system; and d) the 3-body mass $m_{\ell\ell\gamma}$.

We do not expect events with large \cancel{E}_T in the $\ell\ell\gamma$ sample, based on the SM backgrounds; the Run I $ee\gamma\cancel{E}_T$ event was of special interest in the context of supersymmetry [6] due to the large value of \cancel{E}_T (55 ± 7 GeV). Figure 3 shows the distributions in \cancel{E}_T for the $\mu\mu\gamma$ and $ee\gamma$ subsamples of the $\ell\ell\gamma$ sample. No events are observed

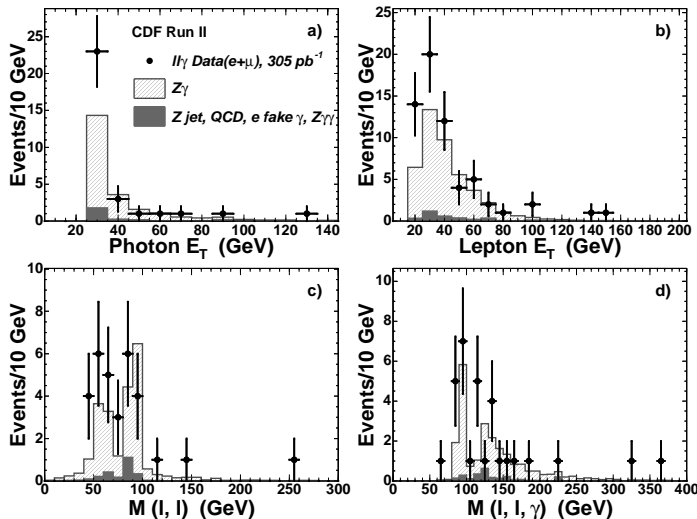


FIG. 2: The distributions for events in the $ll\gamma$ sample (points) in a) the E_T of the photon; b) the E_T of the leptons (two entries per event); c) the 2-body mass of the dilepton system; and d) the 3-body mass $m_{ll\gamma}$. The histograms show the expected SM contributions.

with $\cancel{E}_T > 25$ GeV.

The dominant source of $l\gamma$ events at the Tevatron is electroweak diboson production, in which a W or Z^0/γ^* boson decays leptonically ($l\nu$ or ll) and a photon is radiated from an initial-state quark, the W , or a charged final-state lepton [21]. The number of such events is estimated using leading-order (LO) matrix element event generators [22–24]. Initial state radiation is simulated by

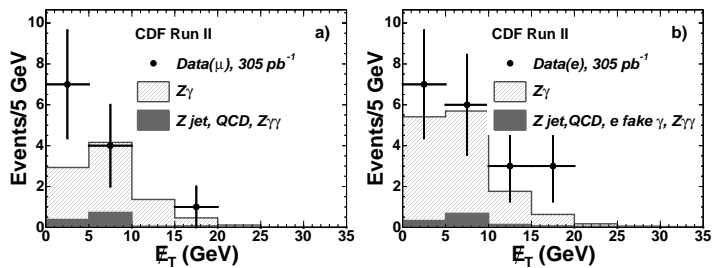


FIG. 3: The distributions in missing transverse energy \cancel{E}_T observed in the inclusive search for a) $\mu\mu\gamma$ events and b) $ee\gamma$ events. The histograms show the expected SM contributions.

the PYTHIA shower Monte Carlo code [25] tuned so as to reproduce the underlying event. The generated particles are then passed through a full simulation of the detector, and these events are then reconstructed with the same reconstruction code used for the data.

The expected contributions from $W\gamma$ and $Z^0/\gamma^* + \gamma$ production to the $l\gamma\cancel{E}_T$ and $ll\gamma$ searches are given in Table I. A correction for higher-order processes (K-factor) that depends on both the dilepton mass and photon E_T has been applied [26]. In the $l\gamma\cancel{E}_T$ signature we expect 22.5 ± 2.8 events from $W\gamma$ and 5.7 ± 1.0 from $Z^0/\gamma^* + \gamma$. In the $ll\gamma$ signature, we expect 20.3 ± 2.4 events from $Z^0/\gamma^* + \gamma$; the contribution from $W\gamma$ is negligible. The uncertainties on the SM contributions include those from parton distribution functions (7%), a comparison of different Monte Carlo generators ($\sim 5\%$), and the luminosity (6%).

High p_T photons are copiously created from hadron decays in jets initiated by a scattered quark or gluon. In particular mesons such as the π^0 or η decay to photons which may satisfy the photon selection criteria. The numbers of lepton-plus-misidentified-jet events expected in the $l\gamma\cancel{E}_T$ and $ll\gamma$ samples are determined by measuring the jet E_T spectrum in $l\cancel{E}_T + \text{jet}$ and $ll + \text{jet}$ samples, respectively, and then multiplying by the probability of a jet being misidentified as a photon, $P_\gamma^{\text{jet}}(E_T)$, which is measured in data samples triggered on jets. The uncertainty on the number of such events is calculated by

TABLE I: A comparison of the numbers of events predicted by the standard model(SM) and the observations for the $\ell\gamma\cancel{E}_T$ and $\ell\ell\gamma$ searches. The SM predictions for the two searches are dominated by $W\gamma$ and $Z^0\gamma$ production, respectively [22–24]. Other contributions come from the tri-boson processes $W\gamma\gamma$ and $Z^0\gamma\gamma$, leptonic τ decays, and misidentified leptons, photons, or \cancel{E}_T .

| Lepton+Photon+\cancel{E}_T Events | | | |
|--|---------------------------------|---------------------------------|---------------------------------|
| SM Source | $e\gamma\cancel{E}_T$ | $\mu\gamma\cancel{E}_T$ | $(e + \mu)\gamma\cancel{E}_T$ |
| $W^\pm\gamma$ | 13.70 ± 1.89 | 8.84 ± 1.35 | 22.54 ± 2.80 |
| $Z^0\gamma^* + \gamma$ | 1.16 ± 0.40 | 4.49 ± 0.64 | 5.65 ± 1.03 |
| $W^\pm\gamma\gamma, Z^0\gamma^* + \gamma\gamma$ | 0.14 ± 0.02 | 0.18 ± 0.02 | 0.32 ± 0.03 |
| $W^\pm\gamma, Z^0\gamma^* + \gamma \rightarrow \tau\gamma$ | 0.71 ± 0.18 | 0.26 ± 0.08 | 0.97 ± 0.22 |
| $W^\pm + \text{Jet faking } \gamma$ | 2.8 ± 2.8 | 1.6 ± 1.6 | 4.4 ± 4.4 |
| $Z^0\gamma^* \rightarrow e^+e^-, e \rightarrow \gamma$ | 2.45 ± 0.33 | - | 2.45 ± 0.33 |
| Jets faking $\ell + \cancel{E}_T$ | 0.7 ± 0.7 | 0.3 ± 0.3 | 1.0 ± 0.8 |
| Total SM Prediction | 21.7 ± 3.4 | 15.7 ± 2.2 | 37.3 ± 5.4 |
| Observed in Data | 25 | 17 | 42 |

| Multi-Lepton+Photon Events | | | |
|--|---------------------------------|--------------------------------|---------------------------------|
| SM Source | $ee\gamma$ | $\mu\mu\gamma$ | $\ell\ell\gamma$ |
| $Z^0\gamma^* + \gamma$ | 12.50 ± 1.53 | 7.81 ± 0.88 | 20.31 ± 2.40 |
| $Z^0\gamma^* + \gamma\gamma$ | 0.24 ± 0.03 | 0.12 ± 0.02 | 0.36 ± 0.04 |
| $Z^0\gamma^* + \text{Jet faking } \gamma$ | 0.3 ± 0.3 | 0.2 ± 0.2 | 0.5 ± 0.5 |
| $Z^0\gamma^* \rightarrow e^+e^-, e \rightarrow \gamma$ | 0.23 ± 0.09 | - | 0.23 ± 0.09 |
| Jets faking $\ell + \cancel{E}_T$ | 0.6 ± 0.6 | 1.0 ± 1.0 | 1.6 ± 1.2 |
| Total SM Prediction | 13.9 ± 1.7 | 9.1 ± 1.4 | 23.0 ± 2.7 |
| Observed in Data | 19 | 12 | 31 |

using the measured jet spectrum and the upper and lower bounds on the E_T -dependent misidentification rate. The misidentification rate is $P_\gamma^{jet} = (6.5 \pm 3.3) \times 10^{-4}$ for $E_T^\gamma = 25$ GeV, and $(4.0 \pm 4.0) \times 10^{-4}$ for $E_T^\gamma = 50$ GeV [21]. The predicted number of events with jets misidentified as photons is 4.4 ± 4.4 for the $\ell\gamma\cancel{E}_T$ signature and 0.5 ± 0.5 for $\ell\ell\gamma$.

The probability that an electron undergoes hard bremsstrahlung and is misidentified as a photon, P_γ^e , is

measured from the control subsample of back-to-back $e\gamma$ events consistent with originating from $Z^0 \rightarrow e^+e^-$ production. The number of misidentified $e\gamma$ events divided by twice the number of ee events gives $P_\gamma^e = (1.7 \pm 0.1)\%$. Applying this misidentification rate to electrons in the inclusive lepton samples, we find 2.5 ± 0.3 and 0.2 ± 0.1 events pass the selection criteria for the $\ell\gamma\cancel{E}_T$ and $\ell\ell\gamma$ searches, respectively.

We have estimated the background due to events with jets misidentified as $\ell\gamma\cancel{E}_T$ or $\ell\ell\gamma$ signatures by studying the total p_T of tracks in a cone in $\eta - \varphi$ space of radius $R = 0.4$ around the lepton track. We estimate there are 1.0 ± 0.8 and 1.6 ± 1.2 events in the $\ell\gamma\cancel{E}_T$ and $\ell\ell\gamma$ signatures, respectively.

We have used both MADGRAPH [22] and COMPEP[24] to simulate the triboson channels $W\gamma\gamma$ and $Z\gamma\gamma$. The expected contributions are small, 0.32 ± 0.03 and 0.36 ± 0.04 events in the $\ell\gamma\cancel{E}_T$ and $\ell\ell\gamma$ signatures, respectively.

Muon backgrounds from hadrons either decaying in-flight or penetrating the iron before the muon chambers, and from the decay of bottom and charm quarks, are found to be negligible.

The predicted and observed totals for both the $\ell\gamma\cancel{E}_T$ and $\ell\ell\gamma$ searches are shown in Table I. We observe 42 $\ell\gamma\cancel{E}_T$ events, versus the expectation of 37.3 ± 5.4 events. In the $\ell\ell\gamma$ channel, we observe 31 events, versus an expectation of 23.0 ± 2.7 events. There is no significant excess in either signature. The predicted and observed

kinematic distributions are compared in Figure 1 for the $\ell\gamma\cancel{E}_T$ signature, and Figures 2 and 3 for the $\ell\ell\gamma$ search.

In conclusion, we have repeated the search for inclusive lepton + photon production with the same kinematic requirements as the Run I search, but with a significantly larger data sample and a higher collision energy. We find that the numbers of events in the $\ell\gamma\cancel{E}_T$ and $\ell\ell\gamma$ subsamples of the $\ell\gamma + X$ sample agree with the SM predictions. We observe no $\ell\ell\gamma$ events with anomalous large \cancel{E}_T or with multiple photons and so find no events like the $ee\gamma\cancel{E}_T$ event of Run I.

We thank the Fermilab staff and the technical staffs of the participating institutions for their vital contributions. Uli Baur, Alexander Belyaev, Edward Boos, Lev Dudko, Tim Stelzer, and Steve Mrenna were extraordinarily helpful with the SM predictions. This work was supported by the U.S. Department of Energy and National Science Foundation; the Italian Istituto Nazionale di Fisica Nucleare; the Ministry of Education, Culture, Sports, Science and Technology of Japan; the Natural Sciences and Engineering Research Council of Canada; the National Science Council of the Republic of China; the Swiss National Science Foundation; the A.P. Sloan Foundation; the Bundesministerium für Bildung und Forschung, Germany; the Korean Science and Engineering Foundation and the Korean Research Foundation; the Particle Physics and Astronomy Research Council and the Royal Society, UK; the Russian Foundation for Basic Research;

the Comisión Interministerial de Ciencia y Tecnología, Spain; in part by the European Community’s Human Potential Programme under contract HPRN-CT-2002-00292; and the Academy of Finland.

-
- [1] F. Abe *et al.* (CDF Collaboration), Phys. Rev. D **59**, 092002 (1999); hep-ex/9806034.
 - [2] F. Abe *et al.* (CDF Collaboration), Phys. Rev. Lett. **81**, 1791 (1998); hep-ex/9801019.
 - [3] D. Toback, Ph.D. thesis, University of Chicago, 1997.
 - [4] Transverse momentum and energy are defined as $p_T = p \sin \theta$ and $E_T = E \sin \theta$, respectively. Missing E_T ($\vec{\cancel{E}}_T$) is defined by $\vec{\cancel{E}}_T = -\sum_i E_T^i \hat{n}_i$, where i is the calorimeter tower number for $|\eta| < 3.6$, and \hat{n}_i is a unit vector perpendicular to the beam axis and pointing at the i^{th} calorimeter tower. We then correct $\vec{\cancel{E}}_T$ for jets and muons. We define the magnitude $\cancel{E}_T = |\vec{\cancel{E}}_T|$. We use the same convention as the Run I analysis: “momentum” refers to pc and “mass” to mc^2 , so that energy, momentum, and mass are all measured in GeV.
 - [5] S.L. Glashow, Nucl. Phys. **22** 588, (1961); S. Weinberg, Phys. Rev. Lett. **19** 1264, (1967); A. Salam, Proc. 8th Nobel Symposium, Stockholm, (1979).
 - [6] See, for example, S. Ambrosanio, G.L. Kane, G.D. Kribs, S.P. Martin, and S. Mrenna, Phys. Rev. D **55**, 1372 (1997); B.C. Allanach, S. Lola, K. Sridhar, Phys. Rev. Lett. **89**, 011801 (2002); hep-ph/0111014.
 - [7] D. Acosta *et al.* (CDF Collaboration), Phys. Rev. Lett. **94**, 101802 (2005).
 - [8] D. Acosta *et al.* (CDF Collaboration), Phys. Rev. D **66**,

- 012004 (2002); hep-ex/0110015.
- [9] D. Acosta *et al.* (CDF Collaboration), Phys. Rev. Lett. **89**, 041802 (2002); hep-ex/0202004.
- [10] J. Berryhill, Ph.D. thesis, University of Chicago, 2000.
- [11] D. Acosta *et al.* (CDF Collaboration), Phys. Rev. D **71**, 032001 (2005).
- [12] F. Abe *et al.* (CDF Collaboration), Nucl. Instrum. Methods A **271**, 387 (1988).
- [13] A. Affolder *et al.*, Nucl. Instrum. Methods A **526**, 249 (2004).
- [14] A. Sill *et al.*, Nucl. Instrum. Methods A **447**, 1 (2000); A. Affolder *et al.*, Nucl. Instrum. Methods A **453**, 84 (2000); C.S. Hill, Nucl. Instrum. Methods A **530**, 1 (2000).
- [15] The CDF coordinate system of r , φ , and z is cylindrical, with the z -axis along the proton beam. The pseudorapidity is $\eta = -\ln(\tan(\theta/2))$.
- [16] S. Kuhlmann *et al.*, Nucl. Instrum. Methods A **518**, 39, 2004.
- [17] The CMU system consists of a central barrel of gas proportional chambers in the region $|\eta| < 0.6$; the CMP system consists of chambers after an additional meter of steel, also for $|\eta| < 0.6$. The CMX chambers cover the region between $0.6 < |\eta| < 1.0$.
- [18] The fraction of electromagnetic energy allowed to leak into the hadron compartment $E_{\text{had}}/E_{\text{em}}$ must be less than $0.055 + 0.00045 \times E_{\text{em}}(\text{GeV})$ for central electrons, less than 0.05 for electrons in the end-plug calorimeters, and for photons, less than $\max[0.125, 0.055 + 0.00045 \times E_{\text{em}}(\text{GeV})]$.
- [19] A. Bhatti *et al.*, submitted to Nucl. Instrum. Methods, Oct. 2005; hep-ex/0510047.
- [20] D. Acosta *et al.* (CDF Collaboration), Phys. Rev. D **71**, 051104 (2005); hep-ex/0501023.
- [21] D. Acosta *et al.* (CDF Collaboration), Phys. Rev. Lett. **94**, 041803 (2005).
- [22] T. Stelzer and W. F. Long, Comput. Phys. Commun. **81**, 357 (1994); F. Maltoni and T. Stelzer, JHEP **302**, 27 (2003); hep-ph/0208156. We designate the production of lepton pairs through the Drell-Yan process, including both the Z^0 and γ amplitudes, as Z^0/γ^* in signatures such as $\bar{p}p \rightarrow Z^0/\gamma^* + \gamma \rightarrow e^+e^-\gamma$.
- [23] U. Baur, T. Han, and J. Ohnemus, Phys. Rev. D **48**, 5140 (1993); J. Ohnemus, Phys. Rev. D **47**, 940 (1993).
- [24] A. Pukhov *et al.*; hep-ph/9908288; E. Boos *et al.* (The COMPHEP Collaboration), Nucl. Instrum. Methods A **534**, 250, (2004); hep-ph/0403113.
- [25] T. Sjostrand, Comput. Phys. Commun. **82** (1994) 74; S. Mrenna, Comput. Phys. Commun. **101** (1997) 232.
- [26] U. Baur, T. Han and J. Ohnemus, Phys. Rev. D **48**, 5140 (1993); U. Baur, T. Han and J. Ohnemus, Phys. Rev. D **57**, 2823 (1998); hep-ph/9710416. Both the $W\gamma$ and $Z\gamma$ K-factors are fixed at 1.36 for generated $\ell\nu$ masses below 76 GeV and for generated $\ell^+\ell^-$ masses below 86 GeV. Above the poles the K-factors grow with E_T^γ to be 1.62 and 1.53 at $E_T^\gamma = 100$ GeV for $W\gamma$ and $Z\gamma$, respectively.